

Planar Two Degree-of-Freedom Legs for Walking Microrobots

Ankur M. Mehta, Kristofer S. J. Pister
Berkeley Sensor and Actuator Center
University of California, Berkeley, CA 94720-1774
mehtank@eecs.berkeley.edu

Abstract—This work presents initial progress towards an autonomous integrated walking microrobot. Design goals include driving a 1 mN (100 mg), 1 cm² device at speeds on the order of 1 cm/s over smooth surfaces. A relatively low complexity MEMS fabrication process is used to create two degree-of-freedom legs to enable a walking gait. Test structures fabricated in this process characterize leg designs and geometries, demonstrating the feasibility of such a microrobot system. A tri-fold flexure based leg can lift a 250 μ N weight 5.5 μ m with a 70 μ N, 15 μ m input actuation, while a hinge based leg can effectively lift a 250 μ N weight 6.5 μ m with a 35 μ N, 15 μ m input actuation.

I. INTRODUCTION

Microscale devices have been under heavy research for decades now, but only recently has there been much progress towards complete microscale systems. The integration of sensing, processing, and communication for instance now allows autonomous sensor motes in a distributed network. However, these are still passive systems, capable of interacting with the environment only within their immediate location. A key element lacking in these microsystems is mobility. Integrated autonomous microrobots, coupling a such a mote with a method of locomotion, can be useful in a variety of surveillance, exploration, and construction tasks.

There are many proposed methods to enable microscale locomotion. Research is underway to develop shuffling, flying, and jumping microrobots. Shuffling robots rely on specific properties of the ground on which they move. Patterned active substrates have enabled some of the smallest mobile devices, but do not allow a fully integrated system and are incapable of interacting with more general environments [1]. Flying is primarily useful for traveling large distances, and often incorporates high energy density hydrocarbon fuels for power [2]. However, such systems are necessarily complex and often lack precise positioning. Jumping microrobots take their cue from insects in nature, storing energy in an elastomer and releasing it quickly to launch them several times their body length [3]. These systems too lack precise positioning, generally using a random walk approach.

This work focuses on enabling walking motion in MEMS microrobots. Walking refers to a method in which the weight of the robot is supported on one set of legs as another set is moved forward off the ground. The weight is then transferred to the second set and the motion repeat. The legs follow periodic non-slip trajectories. This approach is chosen because it enables precise positioning and steering of microrobots on

passive surfaces. It can also be effectively powered by high voltage, low current solar cells. The primary limitation in walking effectiveness is the step size of the legs, requiring surfaces to have roughness features smaller than that size scale.

A walking motion requires at least two dimensions of travel at the foot: the “horizontal” translation which drives the robot forward, and the “vertical” translation which lifts the leg and/or robot from the ground so it can move into position for the next stride. This generally calls for a leg system with at least two degrees of freedom (DOF), either through a single two DOF leg, or a complementary pair of one DOF legs.

Walking microrobots with two single degree-of-freedom legs have been previously developed in [4],[5],[6]. Tethered robots were demonstrated in both [4],[5], with an offboard controller driving an umbilical feeding power directly to the robot legs. These were driven by thermal actuators, resulting in slow, power-hungry legs. A complete system was demonstrated in [6], using solar cells for power with onboard processing for control. The more energy-efficient electrostatic actuators used therein proved incapable of providing sufficient force to overcome losses in the mechanism. These earlier efforts all required complex MEMS fabrication procedures.

A microrobot system is proposed to overcome the problems evident in these earlier attempts. In particular, the primary consideration is a simpler fabrication process. Avoiding heavy process development allows for more attention to mechanism design, with quicker turnaround of design iterations. The design focuses on planar two degree-of-freedom trapezoidal legs to generate the walking motion, actuated by low power electrostatic comb drives. The proposed microrobot system will rely on post-processing assembly to generate the full range of required motions without adding fabrication complexity.

II. SYSTEM DESIGN SPECIFICATIONS

The goal is to create a precision mobility system for sub-centimeter scale sensor motes. As a conservative working point, we can assume the sensor mote payload for such a robot will be a centimeter square silicon die. This is sufficient to incorporate sensing elements, processing and communications circuitry, and solar cells for power. The microrobot system is designed to drive such a payload: the legs in contact with the ground at any given point in the stride must be capable of supporting the entire weight of the robot, while the remaining legs are lifted high enough to overcome surface roughness of

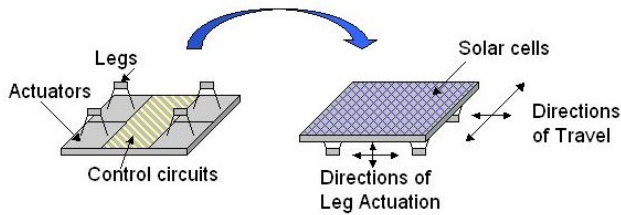


Fig. 1. A conceptual complete microrobot system, with in-plane legs needing to be actuated out-of-plane in order to achieve the desired walking motion.

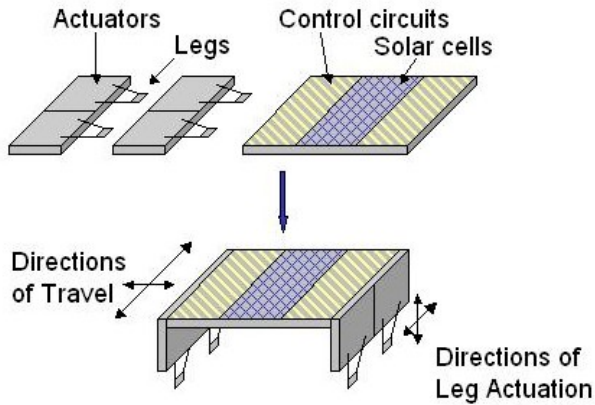


Fig. 2. An alternate system has legs actuated in the plane of their die, with the die rotated to provide the out-of-plane motion.

the ground on which they step. A mass of 100 mg (weighing 1 mN) is chosen as the goal, allowing for the mote payload as well as potential batteries for additional power. Thus the microrobot must be able to support hundreds of μN per leg, with a vertical step height on the order of ten microns.

For a robot to walk across a planar surface, it must have legs capable of moving perpendicular to that plane, clearing the bottom surface of the robot body as it shifts its weight between sets of legs. Thus, if the body is formed horizontally by the substrate, integrated legs must be actuated out-of-plane, as sketched in Fig. 1. Alternately, the legs can be on die independent of the robot body, extending over the edge of the substrate. Then rotating the entire die then enables the legs to drive the robot forward on their side, as in Fig. 2.

The idea of system integration is lucrative, so building the mobility system out of silicon indicates a MEMS approach. A wide variety of MEMS actuators have been studied extensively for various applications; comb drives provide a robust linear actuator with a good tradeoff between force, speed, and displacement at relatively low power consumption. Keeping in mind the robot system design goals, a standard drop-in bidirectional comb drive providing $100 \mu\text{N}$ over a $15 \mu\text{m}$ throw can be used. The leg design must convert the input actuation given by the comb drives into the required output actuation motion.

With a step height of $10 \mu\text{m}$, a heavy 1 mN robot could require up to 10 nJ of output mechanical energy per step if the

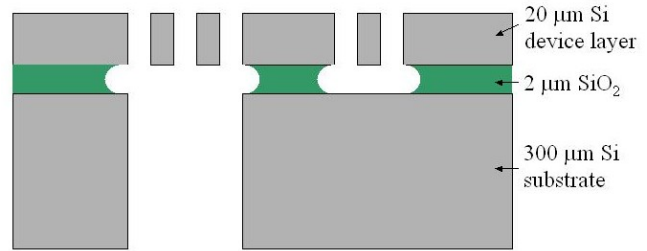


Fig. 3. A simple two mask process is used on an SOI wafer to generate planar structures in the device layer, with backside etching through the substrate.

entire weight of the robot is lifted each step. At an operating frequency of 1 kHz to generate total speeds up to centimeters per second, the mechanical work output would be 10 mW. Reasonable solar cells such as the ones used in [6] can power the efficient comb drives actuating such legs.

III. MEMS FABRICATION

To create a robust and reliable platform for microrobotic device research, a simple fabrication process is desired. Fewer steps requires less process development time, as well as quicker turnaround for device design. A minimal but powerful process is a single layer silicon-on-insulator (SOI) process, where the device layer is patterned and undercut to make planar structures. An additional mask can be used on the backside to clear regions of the substrate. The result of this two mask process is diagrammed in Fig. 3.

The SOI wafer used has a device layer of $20 \mu\text{m}$ with a $2 \mu\text{m}$ buried oxide layer. Devices are patterned in the topside mask, and transferred into photoresist on the device layer through lithography. A silicon deep reactive ion etch (DRIE) is used to cut up to 10:1 aspect ratio trenches, defining the structures. The wafer is flipped and the backside mask is aligned to the front etch and patterned using photolithography. The wafer is then attached to a handle wafer using a thermally conductive compound, and the substrate is etched using DRIE through the backside. A subsequent plasma etch through the backside holes clears those areas of the buried oxide as well. An acetone rinse removes the now-separate die from the handle wafer. These die can be placed in HF for an isotropic oxide etch, releasing and undercutting the structures on the device layer. An anti-stiction coating is applied to ensure smooth operation.

The chosen process imposes restrictions on the design of potential MEMS devices. Only single layer planar geometries are permitted, with minimum feature and gap sizes imposed by lithography and etch resolutions. Nonetheless, many types of actuators and flexure based linkages can still be realized. One marked limitation in this process is the constraint to two dimensions, with structures able to only move in the plane of the silicon. Without introducing additional fabrication steps, post-process assembly can be used to generate 3D structures and out-of-plane motions. Pick-and-place microassembly, as explained in [7], can be used to create individual three-dimensional devices by rotating free-released structures from

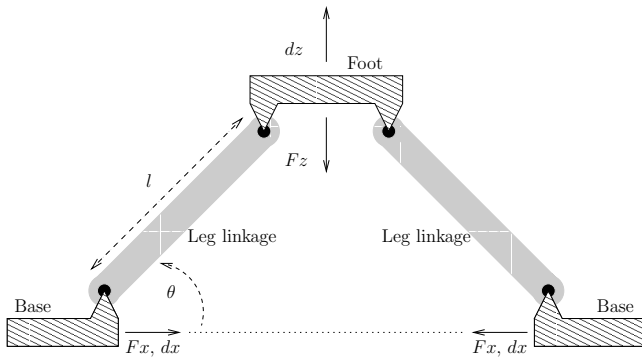


Fig. 4. A schematic of an ideal trapezoidal leg, consisting of rigid members connected by free pivots.

the device layer out-of-plane and clamping them into in-plane structures. Larger scale assembly can also be used to combine discrete MEMS devices in three dimensions through bonding or gluing of their substrates.

IV. TRAPEZOIDAL LEG DESIGN

A walking motion requires two dimensions of travel where a leg contacts the ground, and so a pair of single axis linear actuators can be used. The key development in the walking subsystem design is a trapezoidal leg that provides a linkage connecting two collinear input comb drives to create a two degree-of-freedom output. A schematic of the design is shown in figure Fig. 4. The common mode operation of the comb drives, attached to each base, results in horizontal output travel at the foot, while the differential mode results in vertical displacement. A similar actuator is seen in [8]. The differential input motion is shown in Fig. 5. By driving the two bases out of phase, the foot is driven in a periodic orbit. A pair of such legs can be used to propel a robot forward (Fig. 5d).

The ideal trapezoidal leg design requires the relative rotation of adjacent rigid members to achieve the desired motion. Pivots that rotate freely without inducing a restoring moment cannot be made in a single layer planar process, so alternate linkages have been designed. A tri-fold flexural beam (Fig. 5c) provides the necessary compliance to simulate rotation with a geometrically tunable restoring force. This structure was analytically examined in [9], and proven to provide the required force and displacement output. A flexural leg linkage can however generate large reaction moments and is compliant vertically, inhibiting scaling.

Providing an alternative to the tri-fold flexural beams are rigid beams connected through spring-supported in-plane hinges. These hinges are the two dimensional projections of ideal pivots, with a weak flexure to connect otherwise disjoint elements in plane (Fig. 6). The ball-in-socket joint consists of one one beam ending in a ball rotating within a cylindrical sheath attached to the other beam, as shown in Fig. 7. To avoid the frictional forces generated by the sliding contact between the ball and the socket, a knife-edge joint (Fig. 8) can be used instead. The fabrication process used requires a

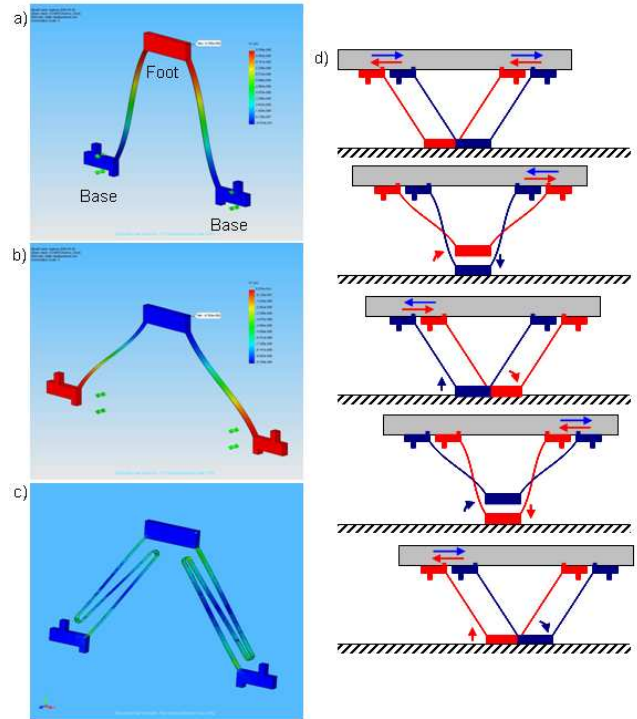


Fig. 5. (a) shows the leg with the independent bases actuated in, raising the foot, while (b) shows the bases actuated out, lowering the foot. If both bases are actuated in the same direction, the foot simply translates. A tri-fold flexural beam (c) is used in the legs to provide additional compliance. Two such legs operating out of phase can be used to propel a robot forward along smooth ground as shown in (d).

minimum gap of $2 \mu\text{m}$, which is responsible for the space between the elements of these hinges.

V. TESTING

Test structures are created to empirically examine these leg linkages. The performance of a leg is defined by four parameters: the load it can support and the step size it can take, with the force and displacement at the base needed to achieve that. The structure shown in Fig. 9 was devised to measure these four values simultaneously. Force gauges with vernier scales are connected to each base and the foot. Micromanipulator probes are used to deflect the gauges at these locations. The resulting forces and displacements can then be read off under a microscope.

The flexure based legs demonstrate the predicted compliance with some additional effects. The folded beam contacts itself at adjacent corners (Fig. 10), increasing the vertical stiffness significantly. This contact additionally prevents the beams from deflecting too far, with the smaller beam angle requiring a smaller reaction moment at the base. Additionally, the bending moment generated by the beam deformation is opposite the torque created on the base by the off-center application of the vertical force. These two counter each other reasonably well, with the support springs in the structure remaining unbuckled.

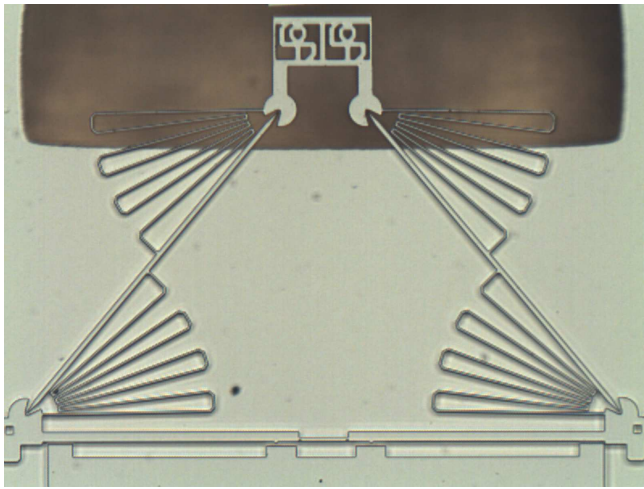


Fig. 6. This leg uses pivots at the edges of a rigid beam, with weak serpentine flexures to keep the pieces in place. The equivalent rotational spring constant of the pivot is lower than the tri-fold beam, but the vertical stiffness is higher.

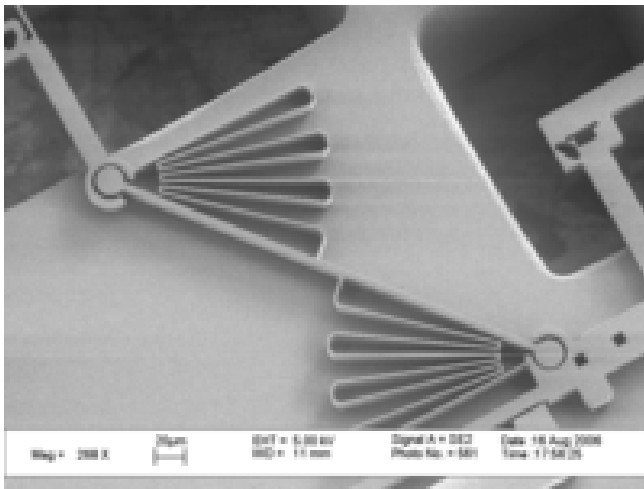


Fig. 7. Pivots can be approximated by a planar ball-in-socket joint. The gap between the ball and socket is the $2\mu\text{m}$ minimum required by the fabrication process.

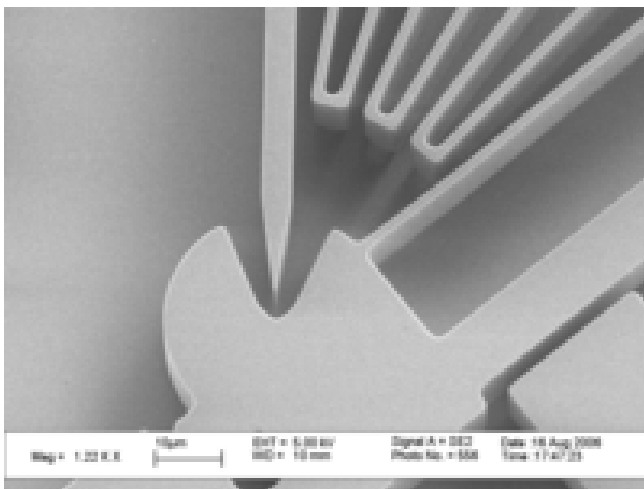


Fig. 8. Knife-edge pivots minimize frictional forces impeding rotation. The edge will sit in the notch upon loading.

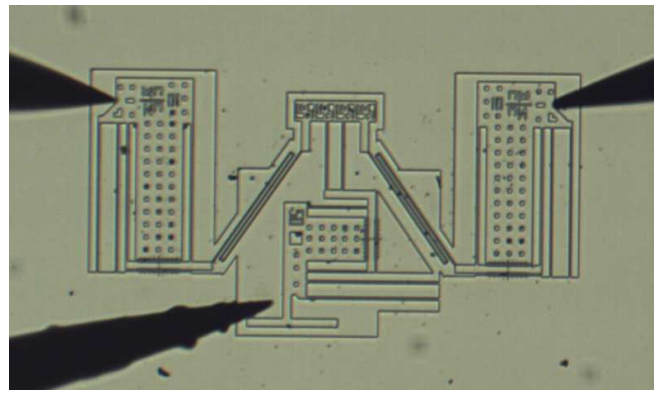


Fig. 9. The test setup used to quantify leg performance. Probe tips are used to apply forces on the bases and the foot, while vernier scales are read to measure the forces and displacements.

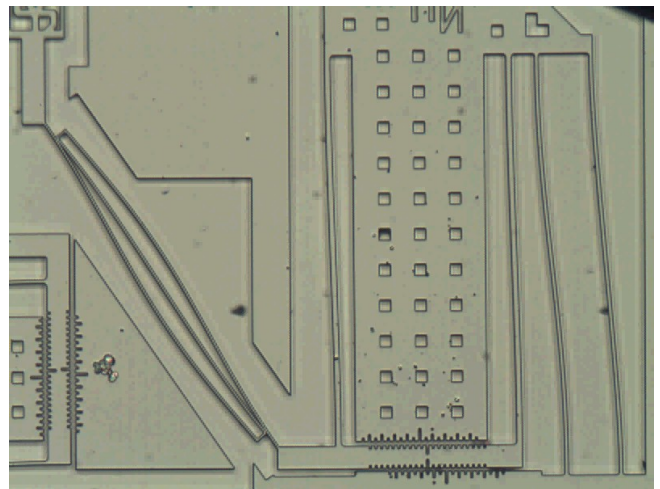


Fig. 10. A tri-fold flexure-based leg test structure fully loaded. The vernier scales can be read to measure the forces and displacements at each node. The graduated hashes on the scale are spaced $5\mu\text{m}$ apart.

The tri-fold leg flexure geometry suggested by the analysis in [9] is shown in Fig. 10 fully loaded. This leg requires a force at the base of $70\mu\text{N}$ over the $15\mu\text{m}$ throw to generate a vertical displacement of $5.5\mu\text{m}$ at the foot given a loading of $250\mu\text{N}$. A lighter loading of $150\mu\text{N}$ on the foot requires an input force of only $25\mu\text{N}$, and generates a vertical displacement of $9\mu\text{m}$ (Fig. 11). This data shows that four of these legs can support and drive a robot weighing up to 1mN using the comb drive specified above. Taking into account the bidirectional actuation of the comb drive, such a robot would take steps $30\mu\text{m}$ long and over $11\mu\text{m}$ high.

The hinged legs as expected display much different behavior. Due to fabrication tolerances, the minimum gap is two μm , and so with a gap in the pivots at each end of the linkage, the legs must compress four microns vertically before supplying any vertical force, as seen in Fig. 12. Thereafter, the legs can be considered vertically rigid. Full loading of a hinged leg takes significantly less force than the tri-fold leg, as seen in Fig. 13. Only $35\mu\text{N}$ input force is required to support 250

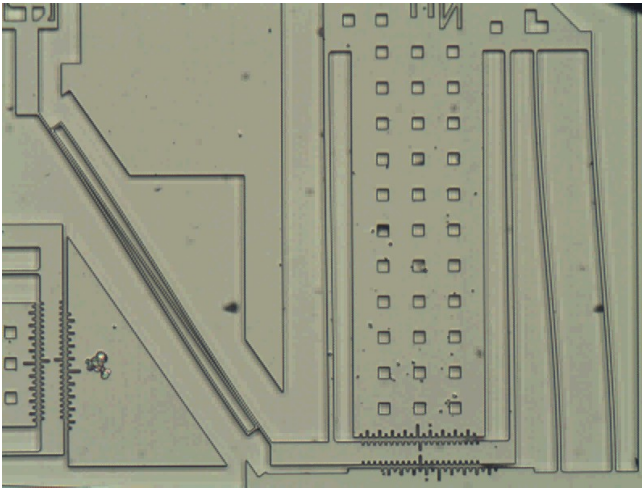


Fig. 11. A lightly loaded tri-fold flexure-based leg.

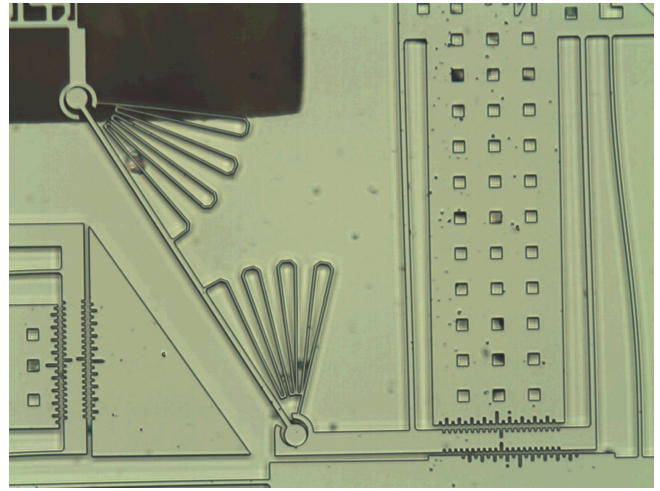


Fig. 13. A fully loaded ball-in-socket joint-based leg.

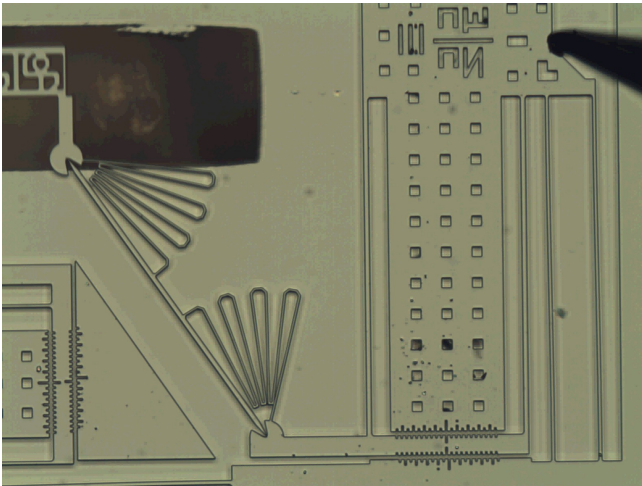


Fig. 12. A knife-edge pivot-based leg test structure requires $4\ \mu\text{m}$ of initial compression to overcome fabrication gaps.

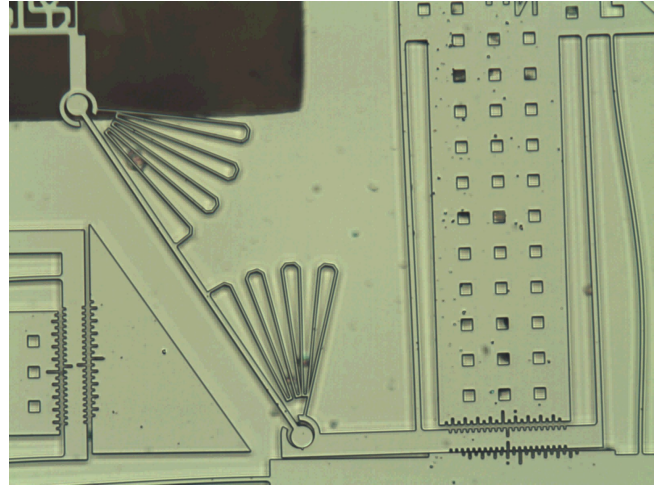


Fig. 14. Increased force at the foot torques the base suspension.

μN on the foot, generating a output displacement of $2.5\ \mu\text{m}$. However, taking into account the initial compression, the net step size for a half gait is $6.5\ \mu\text{m}$. Without a reaction moment due to leg deformation, the torque generated by the off-center vertical loading on the base dominates, and a slight additional force causes the support beams to buckle, twisting the base as seen in Fig. 14.

VI. CONCLUSION

Flexure based legs satisfy the design goals, using the given actuators to lift hundreds of μN a vertical distance of greater than $10\ \mu\text{m}$. However, this design is not scalable; the legs are vertically compliant resulting in a weight-dependent step size. A heavier robot is more restricted in its motion using such legs. Also, increasing the length of the flexure also increases its compliance, to decreasing benefit in step size.

Hinge based legs, on the other hand, scale well. The initial precompression is fixed regardless of size scale, and so becomes less important at larger size scales. A system could

potentially use much larger throw actuators with similar legs to get several times greater step sizes. Furthermore, the legs are vertically rigid after the preload, and so increasing the robot weight should not have an effect on motion provided sufficient input actuation. However, the moment generated by the off-center loading at the bases isn't cancelled, and so heavier robots may torque the actuator suspensions.

The structures fabricated and tested in this work demonstrate the capabilities of a simple SOI process to create two degree-of-freedom legs for a walking microrobot. Both linkage designs satisfy the goals, and the appropriate structure can be chosen for use based on the specifications of the actual system.

ACKNOWLEDGMENTS

This material is based upon work supported under a National Science Foundation Graduate Research Fellowship. The fabrication and process development for this project was done by Sarah Bergbreiter and others in the Pister group.

REFERENCES

- [1] B. Donald, C. Levey, C. McGray, I. Paprotny, and D. Rus, "An untethered, electrostatic, globally controllable MEMS micro-robot," *Journal of Microelectromechanical Systems*, vol. 15, no. 1, pp. 1–15, 2006.
- [2] L. Lindsay, D. Teasdale, V. Milanovic, K. Pister, and C. Pello, "Thrust and electrical power from solid propellant microrockets," in *International Conference on Microelectromechanical Systems (MEMS 2001)*, 2001, pp. 606–610.
- [3] U. Scarfogliero, C. Stefanini, and P. Dario, "A bioinspired concept for high efficiency locomotion in micro robots: the jumping robot grillo," in *IEEE International Conference on Robotics and Automation (ICRA 2006)*, 2006, pp. 4037–4042.
- [4] M. H. Mohebbi, M. L. Terry, K. F. Bohringer, G. T. A. Kovacs, and J. W. Suh, "Omnidirectional walking microrobot realized by thermal microactuator arrays," in *ASME International Mechanical Engineering Congress and Exposition*, New York, NY, 2001.
- [5] T. Ebefors, J. U. Mattsson, E. Kalvesten, and G. Stemme, "A walking silicon microrobot," in *International Conference on Sensors and Actuators (Transducers '99)*, Sendai, Japan, 1999.
- [6] S. Hollar, A. Flynn, S. Bergbreiter, and K. S. J. Pister, "Robot leg motion in a planarized-SOI, two-layer poly-si process," *Journal of Microelectromechanical Systems*, vol. 14, no. 4, pp. 725–740, 2005.
- [7] M. Last, V. Subramaniam, and K. S. J. Pister, "Out of plane motion of assembled microstructures using a single-mask SOI process," in *The International Conference on Solid-State Sensors, Actuators and Microsystems (Transducers '05)*, vol. 1, 2005, pp. 684–687.
- [8] Y.-C. Tung and K. Kurabayashi, "A single-layer pdms-on-silicon hybrid microactuator with multi-axis out-of-plane motion capabilities," *Journal of Microelectromechanical Systems*, vol. 14, no. 3, pp. 548–566, June 2005.
- [9] A. Mehta and K. S. J. Pister, "Flexure-based two degree-of-freedom legs for walking microrobots," in *ASME International Mechanical Engineering Congress and Exposition*, Chicago, IL, 2006.